The Rwenzori Mountains, a Paleoproterzoic crustal shear belt crossing the Albertine rift system

[1]Koehn, [2]D., Link, K., [3]Sachau, T., [3]Passchier, C.W., [4]Aanyu, K., [1]Spikings, A., [1]Harbinson, R.

[1]School of Geographical and Earth Sciences, University of Glasgow, UK, daniel.koehn@glasgow.ac.uk
[2]Guebelin Gem Lab Ltd., Luzern, Switzerland
[3]Tectonophysics, University of Mainz, Germany
[4]Department of Geology and Petroleum studies, Makerere University, Uganda

Abstract This contribution discusses the development of the Paleoproterozoic Buganda-Toro belt in the Rwenzori mountains and its influence on the western part of the East African Rift System in Uganda. The Buganda-Toro belt is composed of several thick-skinned nappes consisting of Archaean Gneisses and Palaeoproterozoic cover units that are thrusted northwards. The high Rwenzori mountains are located in the frontal unit of this belt with retrograde greenschist facies gneisses towards the north, which are unconformably overlain by metasediments and amphibolites. Towards the south the metasediments are overthrust by the next migmatitic gneiss unit that belongs to a crustal scale nappe. The southwards dipping metasedimentary and volcanic sequence in the high Rwenzori mountains shows an inverse metamorphic grade with greenschist facies conditions in the north and amphibolite facies conditions in the south. Early D1 deformation structures are overgrown by cordierite, which in turn grows into D2 deformation, representing the major northwards directed thrusting event. We argue that the inverse metamorphic gradient develops because higher grade rocks are exhumed in the footwall of a crustal scale nappe whereas the exhumation decreases towards the north away from the nappe leading to a decrease in metamorphic grade. The D2 deformation event is followed by a D3 E-W compression, a D4 with the development of steep shear

zones with a NNE-SSW and SSE-NNW trend including the large Nyamwamba shear followed by a local D5 retrograde event and D6 brittle inverse faulting. The Paleoproterozoic Buganda-Toro belt is relatively stiff and crosses the NNE-SSW running rift system exactly at the node where the highest peaks of the Rwenzori mountains are situated and where the lake George rift terminates towards the north. Orientation of brittle and ductile fabrics show some similarities indicating that the cross-cutting Buganda-Toro belt influenced rift propagation and brittle fault development within the Rwenzori mountain and that this stiff belt may form part of the reason why the Rwenzori mountains are relatively high within the rift.

Keywords: East African Rift, Basement, Buganda Toro, Inverse Metamorphic Gradient, Microtectonics, Rwenzori mountains

Introduction

The East African Rift System represents a large zone of crustal extension reaching from the Afar triangle in the north through Ethiopia, Kenya and Tanzania (McConnell, 1972; Morley, 1999; Chorowicz, 2005). Near Lake Victoria the rift system splits into two large branches, an eastern branch that is connected to the Afar triangle and runs east of Uganda through Tanzania and Kenya and a western branch that defines the border between the Democratic Republic of Congo and Uganda and continues through Rwanda and western Tanzania into the Malawi rift. The Albertine rift segment separates the Nubian plate towards the west from the Victoria plate towards the east (Stamps et al., 2008). Several authors argue that the rifts follow zones of weakness in the African crust (McConnell, 1972; Ebinger, 1989; Morley, 1999; Chorowicz, 2005; Ring, 2008).

The east African crust formed during an amalgamation of crustal segments including Archaean basement blocks and several Paleoproterozoic mobile belts (Hepworth and Macdonald, 1966; Stern, 1994; DeWaele et al., 2008). Most of the young rifts and their fault systems seem to follow the Paleoproterozoic basement grain and avoid Archaean terrains, with the northern branch of the East African Rift System following young Proterozoic units (Stern, 1994), the eastern part running along the eastern border of the Archaean Tanzania craton, which also outlines the Victoria plate, and the western branch following the western border of the Tanzania craton (Stern, 1994; Ring et al., 2002; De Waele et al., 2008).

An exception is the Albertine rift that represents the northernmost tip of the western branch of the East African Rift System between Uganda and the Democratic Republic of Congo. Here the young rift runs into Archaean basement and crosses a Proterozoic mobile belt (Link et al., 2010). This part of the rift is subject to extreme topographic variations with rift floors that are 300 to 400 m above sea level with large lakes including Lakes Edward, George and Albert, rift flanks reaching altitudes of more than 3000m as well as the Rwenzori mountains, a basement block within the rift that exceeds 5000m in altitude (Fig. 1; Elliot and Gregory, 1895; McConnell, 1959; Ring et al., 2008). The Albertine rift is branching into the Lake George segment east of the Rwenzori and the Semliki segment west of the Rwenzori. The Lake George segment stops at a basement bridge that is connecting the Victoria plate to the east with the Rwenzori mountains. Seismological and structural studies indicate that the Lake George rift is currently actively propagating northwards towards the Lake Albert rift segment (Lindenfeld et al., 2012). The Semliki rift to the west of the Rwenzoris is connecting the Lake Edward with the Lake Albert segment even though the connection between the Lake Edward and Semliki segments is very narrow (Fig. 1). South of the Rwenzori region the lake Edward rift follows the Midproterozoic Kibaran fold belt (Cahen et al. 1984), which is represented by the low-grade units of the Karangwe-Ankolean system in Uganda (Elliot and Gregory 1895; Link et al. 2010).

In the Rwenzori mountains, the basement consists of a series of gneiss units and metamorphosed units of the Palaeoproterozoic Buganda Toro fold and thrust belt. This Palaeoproterozoic belt has an ENE-WSW strike and crosses the young rift system (McConnell, 1959; Tanner, 1970). The Buganda Toro system is dominating the south-central and western parts of Uganda with an argilitic to arenitic sequence and amphibolites (Schlueter and Trauth, 2008) in between Archaen gneisses. The sequence is generally separated into an amphibolite and marble sequence, an andalusite-cordierite to sillimanite and sometimes biotite schist, meta-tholeiitic lavas and sills and quartzites and conglomerates including the "Toro-quarzites" (McConnell, 1959; Bailey, 1969; Tanner, 1970, 1973; Westerhof et al., 2014). Folding in the units is relatively tight with a dominant ENE trend and a metamorphic grade varying from high grade, which is more dominant in the north to anchi-grade in the south (Schlueter and Trauth, 2008). Even though the sequence in the high Rwenzori was interpreted to be a tight syncline with an overturned southern limb (Mazimhaka, 1973; Westerhof et al., 2014), Link et al. (2010) argue that the Rwenzori mountains represent a southwards dipping dublex system with several crustal scale stacks of basement gneiss with cover sediments and not necessarily a large syncline. Warden (1985) report multiphase deformation with north directed thrusting and E-W compression within the Buganda Toro sequence. North of the Rwenzori mountains the basement is completely made up of Archaean units that belong to the Congo craton (Leggo, 1974). The underlying basement of the Albertine rift system is different from most other parts of the East African Rift system, since the Albertine rift runs into the Archaean craton and is locally branching exactly where the Buganda-Toro belt is situated, which is also the location of the high Rwenzori mountains (Koehn et al., 2008). Link et al. (2010) have argued that the geometry of the rifts around the Rwenzori mountains is a function of the ENE-WSW strike of the Buganda-Toro rocks that hinder straight rift propagation. In addition Sachau et al. (2013) go one step further to argue that the stiff Buganda Toro rocks are directly responsible for the high uplift of the mountains.

In this contribution we study the Buganda-Toro fold belt in the Rwenzori mountains and the surrounding gneisses in detail in order to understand the tectonic evolution of the Palaeoproterozoic mountain belt. In a detailed tectono-metamorphic analysis we unravel the deformation and metamorphic conditions in thin-sections and in the field and present a model of the development of the ductile fabrics. We then compare ductile with brittle fabrics and argue based on geometrical and mechanical considerations that the old geology influences the young tectonic and topographic evolution significantly.

Results

Structure

In this contribution the term Rwenzori mountains refers to the basement block or horst that is situated between the Semiliki and lake George segments of the Albertine rift and that is surrounded by normal faults (Fig.1) including the Bwamba, Riumi-Wasa, Kisomoro and Ibimbo faults. The term central Rwenzori refers to the inset in Fig. 1, which is shown in Fig. 2a and includes the highest peaks, whereas the Rwenzori surroundings represent the rest of the Rwenzori block. The Buganda-Toro units (in green, Fig. 1) cross the Rwenzori mountains from ENE to WSW in two bands. Link et al. (2010) separate the Rwenzori mountains in three distinct units representing a northern gneiss overlain by a first Buganda-Toro unit in the high Rwenzories, a central gneiss unit that over-thrusts the Buganda-Toro unit to the north and is covered by a second Buganda-Toro sequence in the area of the Kilembe mine (KM in Fig. 1) and an over-thrusting southern gneiss unit. The dominant trend of the Buganda-Toro units can also be seen in the strike of the shape fabric in the Archaean gneisses, as indicated with small dotted black lines (Fig. 1). The fabric mainly represents layering and foliation in the gneisses and shows a roughly NE-SW trend to the north of the Rwenzori mountains, parallel to the main rift and horst faults. This trend can also be observed in the southern gneiss unit. Towards the center of the Rwenzori mountains the gneiss fabric changes to a more NE-SW to ENE-WSW orientation. This trend is parallel to the southern boundary of the Buganda-Toro units in the center of the Rwenzori mountains. To the north of the Buganda-Toro units the fabric in the gneiss is cut off by a large shear zone, the Buganda-Toro shear, which is especially prominent on the western side of the central Rwenzori mountains. The Buganda-Toro fabric (indicated with blacks lines in the green units in Fig. 1) trends NE-SW in the central Rwenzories and is folded near Kasese town where it is also offset dextrally by about 10 to 20km along the ductile Nyamwamba shear zone that trends NNE-SSW. Mesoproterozoic Burundien-Karagwe Ankolean or Kibaran rocks (shown in blue in Fig. 1) crop out in the Lake Edward rift segment with possibly a small outcrop east of the Lake George rift segment (Link et al., 2010). Mesozoic to recent sediments and young rift-related volcanic rocks fill the rift. In the following descriptions of the ductile basement rocks we will focus on the central Rwenzori mountains.

In the central Rwenzori mountains the Paleoproterozoic units consist of amphibolites (Fig 2a,b; green unit) and a metasedimentary unit of mainly chlorite, mica, cordierite-andalusite or sillimanite schist, with minor calcsilicates and quartzites (Fig 2a,b; light blue unit). Most of the fabric in the central Rwenzori mountains is dipping towards the south (Fig. 2b). This southwards dip can also clearly be seen in the photograph in Fig. 3a that shows Mount Stanley from the east with a pronounced southwards dipping fabric in the amphibolites (compare with cross section in Fig. 2b).

The fabric in the central gneiss unit in the south in Fig. 2a is aligned parallel to the strike of the Palaeoproterozoic schist unit. Link et al. (2010) interpret this boundary to be a major thrust in a thick-skinned fold and thrust belt where a whole crustal section with the Archaean gneisses at the base is thrust on top of the younger Paleoproterozoic Buganda-Toro schists and amphibolites. In the north of the Buganda-Toro units the Archaean gneiss fabric strikes parallel to the northern schist unit in the eastern part of the map in Fig. 2a whereas in the west the schist unit cuts the gneiss fabric. In this area the gneiss shows a pronounced mylonitic fabric indicating thrusting towards the north (Fig. 3c). The mylonitic fabric is bending into the boundary towards the schist and is displaced dextrally along a brittle fault where the schist unit becomes very narrow. The boundary between the Archaean gneiss and Palaeoproterozoic Buganda-Toro unit probably was an unconformity that was sheared producing the mylonites in the gneisses and later reactivated by a brittle dextral fault.

The Buganda-Toro metasediment and amphibolite sequence in the central Rwenzori mountains shows multiphase deformation and stacking towards the north. Most of the fabric is dipping towards the south with at least six major mylonitic thrust faults that displace different meta-sedimentary and amphibolite units on top of each other (Fig. 2b). The mylonites range from several meters up to tens of meters in thickness. A sequence of metasediments several hundred meters thick lies adjacent to the boundary towards the northern Archaean gneiss (Fig. 2b). Even though the boundary between the Buganda-Toro units and the Archaean gneisses curves from an ENE-WSW to a NNW-SSE trend the dip of the Buganda-Toro units remains consistent. This geometry implies that the curvature of the boundary is not a fold but either represents an unconformity or a faulted contact. The northernmost Buganda-Toro metasedimentary sequence consists of chlorite-schists, quarzites and calcsilicates and is overlain by a small lens of coarse-grained gneiss followed by a 200m thick sliver of amphibolites marking the northern boundary of the Bujuku valley (Fig. 2b). The amphibolite sliver is overthrust by a second metasedimentary unit with a southwards dipping shear zone at the boundary. The second metasedimentary unit is again overthrust by a large amphibolite sequence with a faulted contact. Towards the east a large mylonite can be found within the metasediments that is interpreted to merge with the shear zone marking the boundary between the amphibolite sliver towards the west and the metasedimentary units. The mylonite shows a thrusting sense of movement with a dextral strike slip component (an outcrop picture is shown in Fig. 3d).

The large amphibolite unit on the map in Fig. 2a that hosts the Stanley massif on the west and mount Baker on the east shows a strong southwards dipping fabric with several southwards dipping mylonites that represent thrusting towards the north indicated by SC' fabrics, rotated porphyroblasts, sigma clasts and mineral fishes. These mylonites contain metasediment slivers, such as a quartzite unit below Elena hut (Fig. 3b) and calcsilicate units on the Baker side (Fig. 3e). The southern boundary of the large amphibolite unit is marked by another more than 10 meter thick mylonite zone in the amphibolites overlain by a strongly deformed metasedimentary sequence with cordierte schists, white mica - silimanite schists, calcsilicates and quarzites. This sedimentary unit marks the transition towards the base of the next crustal scale thrust sheet and is overthrusted by the central Archaean gneiss unit.

The lineament map of the high Rwenzori shown in Fig. 2c shows the expression of the main southwards dipping fabric by a WNW-ESE trend of lines. In addition to this trend the lineament map also shows a set of major NNE-SSW and NNW-SSE to N-S trending structures. These represent large steep to vertical faults in the geological map of Fig. 2a that crosscut the southwards dipping sequence in a NNE-SSW and NNW-SSE direction. The three main fabric orientations are also shown in Fig. 2d where a rough trend of the southwards dipping fabric and the two steep N-S running shear zones are shown in great circles. The NNE-SSW trend is parallel to the large Nyamwamba shear that runs just east of the Kilembe mine near Kasese (Fig. 1; marked by Ny).

Fig. 4 shows a detailed compilation of ductile fabrics, mainly foliation and fold axis orientations, that can be found in the Rwenzori mountains, where we compare the orientation of structures within the center of the fold and thrust belt with the orientation of structures further towards the north, south and east. The readings from the center are all taken from the central high Rwenzori mountains represented by Fig. 2 whereas readings from the north, south and east are outside of Fig. 2. Figs. 4a/b show the poles to foliations in the center of the Rwenzori mountains and Rose diagrams of foliation strike, respectively, Figs. 4c/d show the plunge and trend of fold axis of different deformation events and Figs. e/f show poles to foliation and foliation strike in the surroundings of the Rwenzori mountains, mainly in Archaean gneisses in the north and south. We show Rose diagrams of fabric and later on fault strike in order to make a comparison with the lineament map (most of the fabric and fault dip is steep). A comparison of Figs. 4a/b and Figs. 4e/f shows clearly that the southwards dipping fabric is dominating the central Rwenzori mountains whereas the steep NNE-SSW and NNW-SSE trending fabric is dominant in the Rwenzori mountain surroundings. The fold axes shown in Fig. 4c and d show a well-defined plunge towards the SW, even though the data is a mix of 3 folding phases.

Fig. 5 shows the brittle fabric as poles to fault planes and Rose diagrams of fault strike with another separation of the central Rwenzori mountains from its surroundings. The brittle data shown here consists only of distinct fault planes. Fig. 5b of the Rwenzori mountain surroundings shows a clear dominance of steep rift related faults with a NNE-SSW trend parallel to the overall trend of the Lake Albertine rift system (Fig. 1). A small number of faults strike NW-SE, and these are described as transection faults in Koehn et al. (2010) and are defined as fault sets that cut through the Rwenzori mountains at a high angle relative to the main rift faults. On a large scale these transection faults define the trend of the Mubuku valley north of Kasese in Fig. 1. In the central Rwenzori mountains the fault trend changes with the transection faults becoming dominant in addition to the appearance of an EW trending set of faults with a southwards dip.

This second fault trend is similar to the main ductile fabric trend that also dips towards the south. A third NNE-SSW trend of steep faults is in accordance with the rift parallel faults of Fig. 5a/b. The lineament map of the central Rwenzori mountains in Fig. 2c also shows the EW trend of the main ductile fabric and the NNE-SSW and SSE-NNW trend of the steep faults.

Metamorphism

In order to understand the tectonometamorphic history of the Buganda-Toro units and the Archaean gneisses in the central Rwenzori mountains, we studied the mineral assemblages of the Archaean gneisses at the boundaries of the Palaeoproterozoic belt and mineral assemblages of the different schist units in detail. Fig. 6 shows structures within the gneiss units near the tectonic contact in the north and the thrust fault in the south. The thin sections show clearly that the northern and southern gneiss are very different, with Fig. 6a showing a thin section of the southern gneiss and Figs. 6b and c the northern gneiss with Fig. 6c the mylonite fabric in the northern gneiss. The gneiss in the south shows very large grain sizes with grain diameters of typically 1 to 5 mm, lobate grain boundaries indicating grain boundary migration in quartz and feldspar and distinct subgrain patterns in quartz crystals including chessboard subgrain patterns. Lobate grain boundaries and chessboard subgrain patterns as well as the large grain size are all typical indicators of high temperature deformation within the gneisses (500 to 600 degrees, indicating amphibolite facies or higher; Passchier and Trouw, 2005). By contrast the mylonitic and non-mylonitic gneisses in the north are fine-grained with brittle feldspar porphyroclasts whereas quartz shows fine crystallized fabric indicating subgrain rotation and bulging recrystallization (Passchier and Trouw, 2005). The northern gneisses contain 40 to 50 percent of a very fine-grained matrix with small micas, quartz and feldspar. Overall the metamorphic grade in the northern gneisses seems to be greenschist facies (300 to 400º). The mylonite shown in Fig. 6c was also active under greenschist facies conditions.

The schist units north and south of the central Rwenzori Buganda-Toro units show a similar pattern to the gneisses. In the north at the boundary to the Archaean gneisses the schist units show lower greenschist facies grade. The grain size is very small with minor growth of micas. Towards the main amphibolite unit the schists in the north show first growth of albite and the shear zone shown in Fig. 3d shows typical structures indicating greenschist facies deformation conditions with porphyroclastic feldspars and small recrystallized quartz ribbons. In contrast the schist in the south of the large amphibolite units shows porphyroblasts of cordierite and andalusite several centimetres in diameter (Fig. 7a,b; Fig. 8a,b) and local fibrolitic sillimanite (Fig. 8c) and pronounced late muscovite growth (Fig. 8a-d). Overall the metamorphic grade is much lower in schist and gneisses in the north than in the south, with high grade amphibolite facies conditions in the schist and even higher grade in the gneisses. Since the main fabric is dipping towards the south the Buganda-Toro sequence in the central Rwenzori mountains shows an inverted metamorphic grade.

Tectonometamorphic history

In the central Rwenzori mountains we define 6 deformation stages within the Buganda Toro units and relate them to different metamorphic conditions. Fig. 8f shows a summary for the high-grade schist to the south of the large amphibolite unit in the central Rwenzori mountains where the growth of different metamorphic minerals is shown in relation to the different deformation phases. Phase D1 is represented by early isoclinal folds in quarzite and schist of the Palaeoproterozoic units. Some deformation of the Archaean gneiss units may predate D1, this deformation may then be called D0. D1 folds are shown in Fig. 2a (marked as F1) with intermediate plunges of 30 to 45 degrees. Metamorphic conditions that are associated with D1 show early Muscovite and Biotite growth as well as growth of cordierite and andalusite. D1 structures are completely overprinted and rotated by the D2 event and are mostly transposed. D2 is the main event in the area and is represented by the southwards dipping fabric and the major southwards dipping shear zones that record northwards directed thrusting. It is not clear if the mylonite in the Archaean gneisses north of the northern schist unit belongs to D2 or if this is an older event since the mylonite is cut off by the boundary to the metasediments. The metamorphic grade and displacement direction of the mylonitic gneiss fit the general D2 trend and the metamorphic condition in the north (northwards directed thrusting under greenschist facies conditions), indicating that the mylonite may be part of the D2 thrusting. An S2 cleavage is well developed within the Buganda-Toro sequence and shows again the southwards directed dip parallel to the main fabric. D2 folds (F2 in Fig. 2) are asymmetric with a northwards vergence being consistent with the northwards directed thrusting and show shallow plunging fold axes. Metamorphic conditions that are associated with the D2 event vary across the study area with greenschist facies mineral growth in the northern schist (growth of albite, chlorite, small muscovite) and amphibolite facies conditions in the southern units with the growth of muscovite, cordierite, andalusite, sillimanite and garnet. Fig. 7 shows a close-up of the interference of D1 and D2 structures in the southern schist. Fig. 7b shows a typical cordierite porphyroblast that is overgrowing an S0 fabric that represents layering or bedding in the schist. This early fabric was folded with an associated S1 foliation before it was overgrown by the porphyroblast, indicating either intertectonic growth between D1 and D2 or syntectonic growth at a late D1 stage. D2 foliation and associated folds outside the porphyroblast fold the S1 foliation and are associated with the major northwards directed thrusting event indicated by the northwards vergence of the minor folds. The interference of S1 and S2 and an example of a small scale isoclinal D1 fold (F1) can be seen in the thin section of Figs. 7c and d. The isoclinal D1 fold is associated with a flat lying S1 cleavage that can only be seen in the hinge of the D1 fold. The S2 cleavage appears towards the lower right hand side of the section and shows only minor folding of either S1 or S0.

Fig. 8a shows another relation of mineral growth and deformation phases where a cordierite porphyroblast overgrows a D1 fold. The relation is similar to the one shown in Fig. 7a/b where cordierite also overgrows D1 structures. The cordierite is then itself overgrown by large white mica crystals. The same relation is shown in Fig. 8b where cordierite and andalusite overgrow a D1 fabric with a slight crenulation or kinks. Again late white mica crystals overgrow the earlier porphyroblasts. Fig. 8c shows fibrolitic sillimanite growth during the later D2 stage, accompanied by late garnet growth. After stage D2 white mica continues to overgrow the fabric during D3 to D5 stages. D3 is associated with an E-W compression of the area that produces D3 folds (F3 in Fig. 2) and an S3 foliation. This deformation is mainly seen in the relatively weak schist that is refolded. The S3 foliation is gently east-dipping, while F3 fold axes plunge gently towards the south. The D3 event postdates the main metamorphic event in the schist. D3 folds are offset by D4 sub-vertical shear zones with a NNE-SSW and NNW-SSE strike that show displacements that range from strike slip to dip slip. A large number of the strike slip shear zones are dextral in accordance with the dextral movement of the large Nyamwamba shear in the eastern Rwenzori mountains that may also represent a D4 event: The Nyamwamba is clearly offsetting folds in the Kilembe mine area that refold the D2 folds and are thus classified as D3 structures. However, the plunge of the D3 fold axis near Kilembe mine is mostly towards the SSE instead of the SSW plunge that is found in the central Rwenzori mountains. D5 is a minor event with an S5 foliation that strikes N-S to NNW-SSE and a series of kink bands (Fig. 8e). The age relation between D5 and D4 is not clear. We place D5 after D4 since D5 shows retrograde metamorphic conditions with chlorite growth. Finally D6 is represented by a series of brittle events with a pronounced set of brittle reverse faults indicating NNW directed shortening in the east of the central Rwenzori mountains as shown in Fig. 2a and Fig. 3f. Whether or not this brittle reverse faulting event is rift related and is associated with the uplift of the mountain or whether it is a much older event is not clear.

Fig. 8f shows a summary of the deformation events and related mineral growth for the schist in the southern part of the amphibolites in the central Rwenzori mountains. D1 is associated with a muscovite and biotite growth event and at a late stage in D1 cordierite grows and is followed by growth of andalusite. D2 is associated with white mica growth and cordierite growth in the early stages of D2. Andalusite continues to grow at later stages in D2 followed by sillimanite and finally garnet at the end of the D2 deformation. Stages D3-D5 are retrograde events with muscovite and chlorite growth and in stage D6 deformation becomes brittle.

Discussion

We interpret the structures and metamorphic sequences following the model of Link et al., (2010). The northern gneisses in the study area seem to represent a shallower crustal level than the southern gneisses. According to the Link et al. (2010) model, the gneiss-metasediment units represent large crustal-scale thrust sheets where the central Rwenzori mountains represent the first (northernmost) sheet that was over-thrust by the southern gneiss. That means that the gneisses in the north are recording an intermediate level of depth, which represents the actual gneiss-metasediment unconformity, whereas the gneisses in the south represent the base of a 10km thick gneiss sheet and thus were exhumed from a much deeper level. This can be clearly seen by the much higher metamorphic grade in the southern gneiss in comparison to the greenschist facies northern gneiss. The observed dominant northwards directed thrusting of the D2 event also fits well with the idea that the Buganda-Toro belt represents several northwards directed thrust sheets. However, this does not explain the inversion of the metamorphic grade that we find with low-grade schist at the base of the Buganda-Toro sequence near the unconformity to the northern gneisses and the high grade schist at the top of the section just below the next gneiss thrust sheet. A possible interpretation of these findings is shown in Fig. 9 that represents a schematic cross section through the central Rwenzori mountains. If we consider that the whole Palaeoproterozoic sequence at the top of the Rwenzori mountains is a large-scale shear zone in the footwall of a major thrust, the units in the north show a much smaller displacement than the units in the south of the section. The sketch in Fig. 9 illustrates that we can exhume rocks that were 15km deeper in the crust in the south directly in the footwall of the major thrust where the next crustal scale imbrication is thrusted northwards compared to those in the north. The low grade schist in the north is from the front of the orogenic belt and does not experience large-scale crustal loading, which brings them in the greenschist facies zone. The units in the south however come from a deeper part of the orogenic belt so that they first experience crustal loading due to an initial stacking of the sequence that probably led to the development of D1 structures and growth of the first metamorphic minerals at a later D1 stage. Subsequently, the continuous northwards directed thrusting led to the continuous transport of these rocks in the footwall of the large crustal scale thrust towards the north and finally their exhumation. D2 and associated mineral growth show this stage of progressive shearing with high strain in the footwall of the major thrust. After exhumation D3 deformation progressed under retrograde conditions. Whether or not all D3 to D5 structures belong to the Palaeoproterozoic event is not completely clear. However, the Mesoproterozoic rocks found south of the Rwenzori mountains show a very low grade metamorphism (Link et al., 2010) indicating that D3 and D4 may have taken place before the Midproterozoic.

If we compare the presented deformation phases with those of Link et al. (2010), D1 of Link et al. (2010) describes deformation in the gneisses prior to the Palaeoproterozoic deformation, so that D1 of Link et al. (2010) could be called D0 in our case. D1 of our model is not mentioned in Link et al. (2010), D2 and D3 of Link et al. (2010) and D2 and D3 presented in this contribution are the same events whereas D4-6 is not described in Link et al. (2010). However, Link et al. (2010) describe a D4 event that represents the Mesoproterozoic Kibaran orogeny, which may correspond with the D5 presented here or even the D6 brittle reverse faulting that we find. Delvaux et al. (2012) describe a late Panafrican compression event and a Triassic strike slip event in the Rukwa rift, which may correspond to the D6 event that we find in the Albertine rift.

Reactivation and rift faults

Brittle faults (Fig. 5) and the ductile foliations (Fig. 4) have a similar trend, especially within the central Rwenzori mountains. However, the structures are not completely identical, the main brittle fault strike outside the central Rwenzori mountains is rift parallel with a major NNE-SSW strike whereas the main ductile foliation strike is NNW-SSE. In the center of the Rwenzori mountains the ductile deformation is dominated by a S to SSE dipping foliation whereas the brittle faulting shows a more S to SSW dip. In addition steep NNW-SSE and NNE-SSW brittle faults are almost missing in the ductile fabric. In summary we can observe some reactivation of old ductile fabrics by younger faults but this is not always the case, the young rift faults can also dominate the pattern with new directions. This is also seen in the field where some of the ductile shear zones are cut by young active faults at very low angles of 10 degrees without major reactivation of the old fabric. However, two major influences of the ductile on the brittle fabric can be established:

1) the WSW-ENE strike of the Buganda-Toro units and the associated southwards dipping fabric are exploited by brittle faults and this trend may influence rift propagation and

2) the stiff amphibolite unit is dipping towards the south and may go down to depths of more than 10km (Fig. 13; in Link et al. (2010)). This is in accordance with the model of Sachau et al. (2013) where the Rwenzori mountains are modeled as a stiff block that is uplifted with the whole rift system including the Semliki and lake George rift.

Note that amphibolite can be an extremely strong rock that is hard to erode (Passchier and Trouw, 2005). An amphibolite body that is as large as the one exposed in the central Rwenzori mountains represents a significant anomaly in the crust. This body leads to a deflection of the propagating rifts and the capturing of the Rwenzori mountains by the rifts (Koehn et al., 2010). In addition it is stiff enough to influence the elastic behavior of the crust in accordance to the model of Sachau et al. (2013). The stiff block can connect the Semliki and Lake George rift so that they act together as one wide rift and this leads to an uplift of the mountain in the middle of the rift. The lack of a root below the mountains, which is expressed by a high-lying crust-mantle boundary below the Rwenzori mountains (Woelbern et al., 2010), also supports these uplift models, with the Rwenzori mountains being uplifted within the middle of the rift.

Conclusions

The Buganda-Toro units in the central Rwenzori mountains represent a large-scale shear zone below an over-thrust gneiss unit at the front of a large Palaeoproterozoic orogeny with northwards directed displacement of several thick skinned thrust imbricates. The frontal Palaeoproterozoic units show lower greenschist facies conditions and overly retrograde gneiss units unconformably. The main deformation within the Palaeoproterozoic sequence is represented by thrusting towards the north along several shear zones in addition to north-vergent folds. In the central Rwenzori mountains the metamorphic gradient is inverse with lower greenschist facies grade in the northern units and high grade amphibolite facies conditions in the southern units in the footwall of a crustal-scale shear zone that exhumes migmatitic gneisses at the base of the next crustal-scale imbrication. The inverse gradient develops because deformation increases strongly towards the south so that the whole belt in the footwall of the next crustal scale thrust is sheared with a southwards increase in displacement and thus increase in exhumation. In the south metamorphic minerals indicate a D1 event that starts prior to the D2 thrusting and continues within D2 representing loading of the southern thrust sheets on top of the sequence before it becomes exhumed along the southern shear zone. The sequence is then folded during E-W compression (D3), displaced along steep NNE-SSW and NNW-SSE trending shear zones (D4), deformed by an additional minor event (D5) and later on overprinted by brittle reverse faulting (D6). A comparison of brittle faults and ductile fabric indicates that the old fabric influences rift related faults especially in the vicinity of the central Rwenzori mountains, where steep ductile shear zones are reactivated by brittle faults. We propose that the Buganda-Toro belt that crosses the rift influences rift propagation and that its stiffness, especially the large amphibolite block in the center, may help to explain the anomalously hight of the Rwenzori mountain.

Acknowledgements

We are very grateful for the suggestions of the reviewers Ruediger Killian and Enrique Gomez Rivas, which significantly enhanced the quality of the manuscript. We acknowledge funding of our research by DFG grant KO 2463/4-2 of the Forschergruppe "Rift Dynamics, uplift and climate change in Equatorial Africa." we thank the Uganda Wildlife Authority for their permission to work in the parks and the Ugandan National Council of Science and Technology. We acknowledge the use of the program Stereonet 6.3.2 from R.W. Allmendinger.

References

Bailey, A. I. 1969. Report on the geology of the Watamagufu-Bugoye area of the Ruwenzori Mountains. 13th Ann. Rept. Inst. Afr. Geol. Univ. Leeds, 13–14.

Cahen L, Snelling NJ, Delhal J, Vail JR (1984) The geochronology and evolution of Africa. Clarendon Press, Oxford

Chorowicz, J., 2005, The East African rift system: Journal of African Earth Sciences, v. 43, n. 1–3, p. 379 – 410, http://dx.doi.org/10.1016/j.jafrearsci.2005.07.019

Delvaux D., Kervyn, F., Macheyeki, A.S., Temu, E.B. (2012) Geodynamic significance of the TRM segment in the East African Rift (W-Tanzania): Active tectonics and paleostress in the Ufipa plateau and Rukwa basin. Journal of Structural Geology, 37, 161-180

De Waele B, Johnson SP, Pisarevsky SA (2008) Paleoproterozoic to Neoproterozoic growth and evolution of the eastern Congo Craton. Its role in the Rodenia puzzle. Precambrian Res 160(2):127–141

Ebinger, C. J., 1989, Tectonic development of the western branch of the East African rift system: Geological Society of America Bulletin, v. 101, n. 7, p. 885–903, http://dx.doi.org/10.1130/0016-7606(1989)1010885:TDOTWB2.3.CO;2

Elliot GFS, Gregory JW (1895) The geology of Mount Ruwenzori and some adjoining regions of equatorial Africa. Quart J Geol Soc 51:669–680

Hepworth JV, Macdonald R (1966) Orogenic belts of the northern Uganda basement. Nature 210:726–727

Koehn D, Aanyu K, Haines S, Sachau T (2008) Rift nucleation, rift propagation and the creation of basement micro-plates within active rifts. Tectonophysics 458:105–116

Koehn, D., Lindenfeld, M., Ruempker, G., Aanyu, K., Haines, S., Passchier, C. W., and Sachau, T., 2010, Active transsection faults in rift transfer zones: evidence for complex stress fields and implications for crustal fragmentation processes in the western branch of the East African Rift: International Journal of Earth Sciences, v. 99, n. 7, p. 1633–1642, http://dx.doi.org/10.1007/s00531-010-0525-2

Leggo PJ (1974) A geochronological study of the basement complex of Uganda. J Geol Soc Lond 130:263–277

Lindenfeld, M., Ruempker, G., Link, K., Koehn, D., and Batte, A., 2012, Fluid-triggered earthquake swarms in the Rwenzori region, East African Rift—Evidence for rift initiation: Tectonophysics, v.566–567, p. 95–104, http://dx.doi.org/10.1016/j.tecto.2012.07.010

Link, K., Koehn, D., Barth, M. G., Tiberindwa, J. V., Barifaijo, E., Aanyu, K., and Foley, S. F., 2010, Continuous cratonic crust between the Congo and Tanzania blocks in western Uganda: International Journal of Earth Sciences, v. 99, n. 7, p. 1559 –1573, http://dx.doi.org/10.1007/s00531-010-0548-8

MacDonald R (1966) Geological map of Uganda. Department of Geological Survey and Mines, Uganda.

Mazimhaka, P. K. (1973) Report on a study of part of the eastern deposit at Kilembe mines Limited.Unpubl. Econ. Geol. Proj. Rept. 1–33, Kampala.

McConnell R. B. (1959) Outline of the geology of the Ruwenzori 564 Mountains. Overseas Geol Miner Resour 7:245–268 565

McConnell, R. B., 1972, Geological development of the rift system of eastern Africa: Geological Society of America Bulletin, v.83, n.9, p.2549–2572, http://dx.doi.org/10.1130/0016-7606(1972)83[2549: GDOTRS]2.0.CO;2

Morley CK (1999) Geoscience of rift systems-evolution of East 568 Africa. AAPG stud geol 44:242

Passchier C.W. and Trouw R. (2005) Microtectonics, Springer, 366pp.

Ring U (2008) Extreme uplift of the Rwenzori Mountains in the East African rift, Uganda: structural framework and possible role of glaciations. Tectonics 27: TC4018, doi:10.1029/2007TC002176

Schlueter, T., Traut, M. (2008) Geological Atlas of Africa. Springer Berlin-Heidelberg, 320 pp.

Sachau, T., Koehn, D., Passchier, C.W. (2013) Mountain-building under extension. American Journal of Science, 313 (4).

Stamps DS, Calais E, Saria E, Hartnady C, Nocquet JM, Ebinger CJ, Fernandes RM (2008) A kinematic model for the East African rift. Geophys Res Lett 35:L05304

Stern RJ (1994) Arc assembly and continental collision in the neoproterozoic east African orogen: implications the consolida- tion of Gondwanaland. Annu Rev Earth Sci 22:319–351

Tanner (1970) The Ruwenzori Fold Belt of East Africa. Ann Rep Res Inst. African Geology University Leeds, 14:3–7

Tanner, P. W. G. (1973) Regional metamorphism of low pressure intermediate type in the Ruwenzori fold belt of East Africa. Ann. Rept. Res. Inst. Afr. Geol., Univ. Leeds 17, 20–26.

Warden, A. J. (1985) Reappraisal of the geological setting and potential of Kilembe copper mine, Uganda. Trans. Instn. Min. Metall., Section B, B94–B105.

Westerhof, A.B.P., Haermae, P., Isabirye, E., Katto, E., Koistinen, T., Kuosmanen, E., Lehto, T., Lehtonen, M.I., Maekitie, H., Manninen, T., Maenttaeri, I., Pekkala, Y., Pikki, J., Saalmann, K., Virransalo, P. (2014) Geology and Geodynamic Development of Uganda with Explanation of the 1:1,000,000 – Scale Geological Map, Geological Survey of Finland, Special Paper 55.

Wölbern, I., Rümpker, G., Schumann, A., Muwanga, A., (2010) Crustal thinning beneath the Rwenzori region, Albertine rift, Uganda, from receiver-function analysis. International Journal of Earth Sciences (Geologische Rundschau) 99, 1545–1557.

Figure Captions

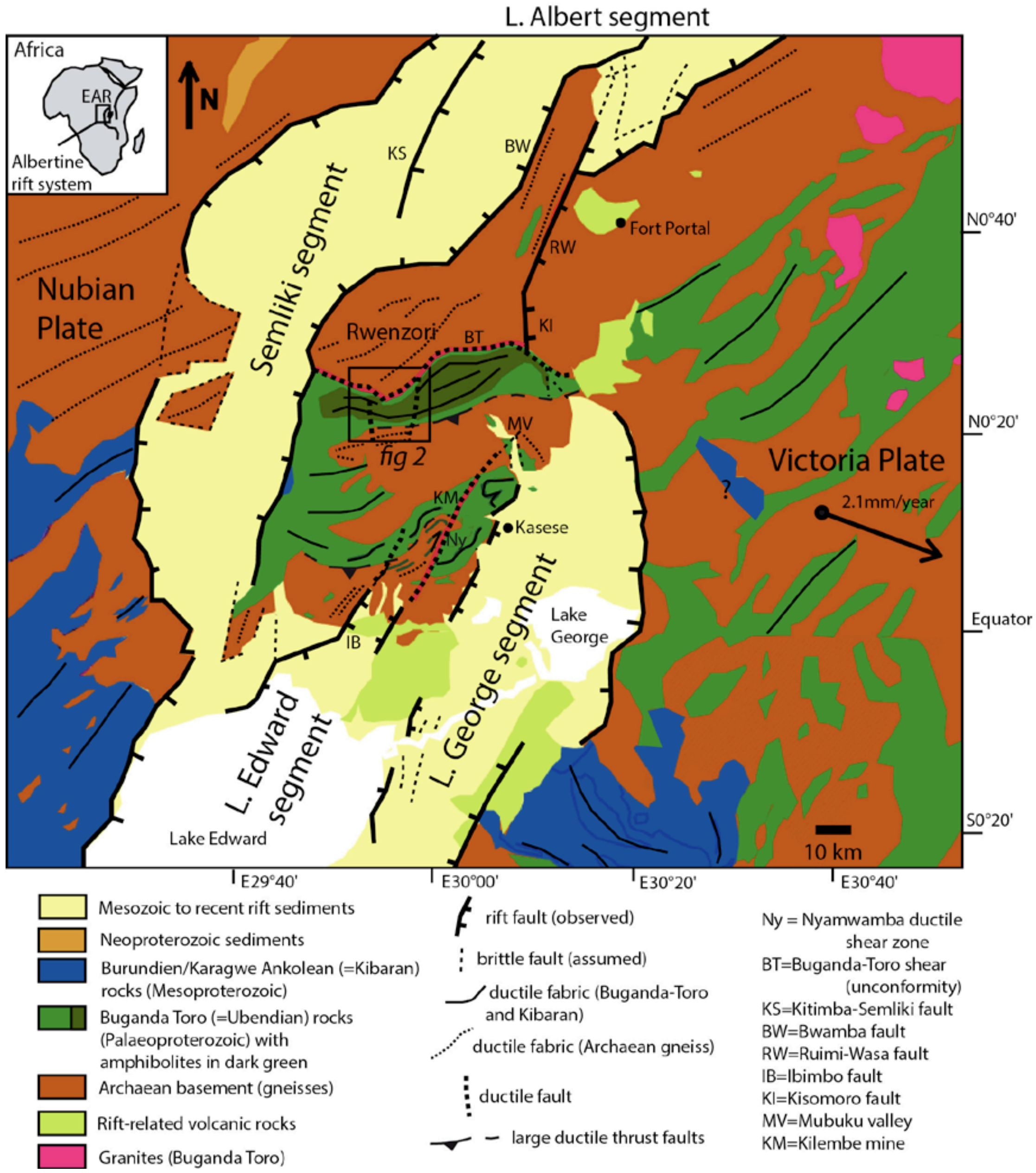

Figure 1 Overview of the geology of the southern part of the Albertine rift system around the Rwenzori mountains after MacDonald (1966) Koehn et al. (2010); Link et al. (2010) and Lindenfeld et al. (2012). Faults are shown in black lines, and basement fabric is shown in dotted lines. Arrow on the right hand side of the map shows the movement of the Victoria plate east of the rift relative to the Nubian plate left of the rift after Stamps et al., (2008). The box in the center of the Rwenzori mountains shows the position of Fig. 2.

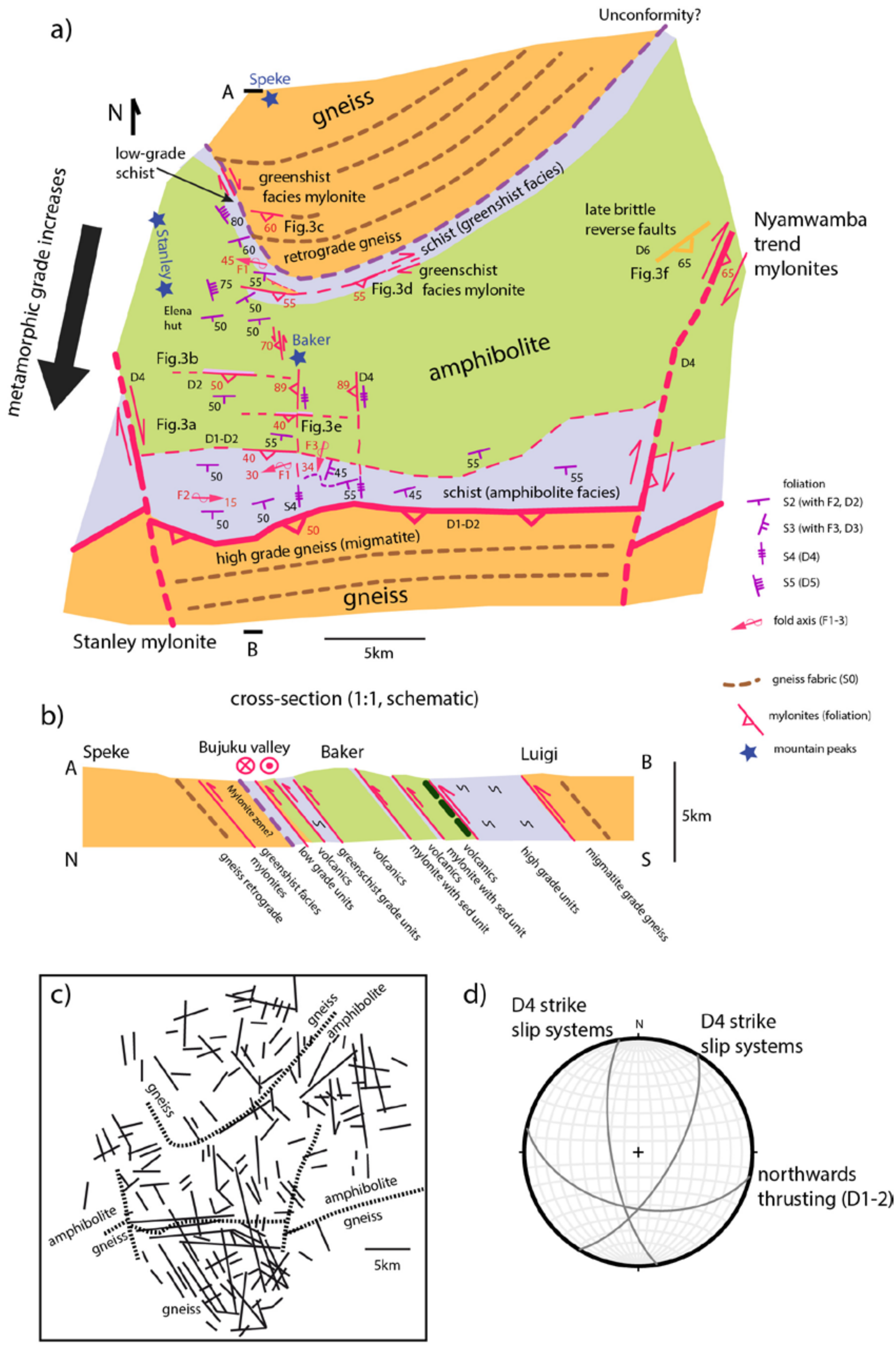

Figure 2 a) Detailed map of the central high Rwenzori with the main structural components. The high Rwenzori are dominated by a large amphibolite body surrounded by metasedimentary units containing mainly schist belonging to the

Paleoproterozoic Buganda-Toro unit. The south and north are dominated by Archaen gneisses. The main fabric in all of the units dips toward the south and is cut by steep NW-SE and NE-SW striking faults. b) Schematic cross section through the map shown in a) in a N-S direction from A to B. The cross section also shows the dominantly southwards dipping fabric and a dominant north directed stacking of units. c) Lineament map of the high Rwenzori with the main gneiss-schist boundary in dotted lines based on the interpretation of Aster satellite images. The lineaments clearly show the NW-SE to N-S trend of steep structures. d) Stereoplot of the main fabric with the dominant features showing the northwards directed thrusting and main fabric and two NNW-SSE and NNE-SSW directed steeps faults.

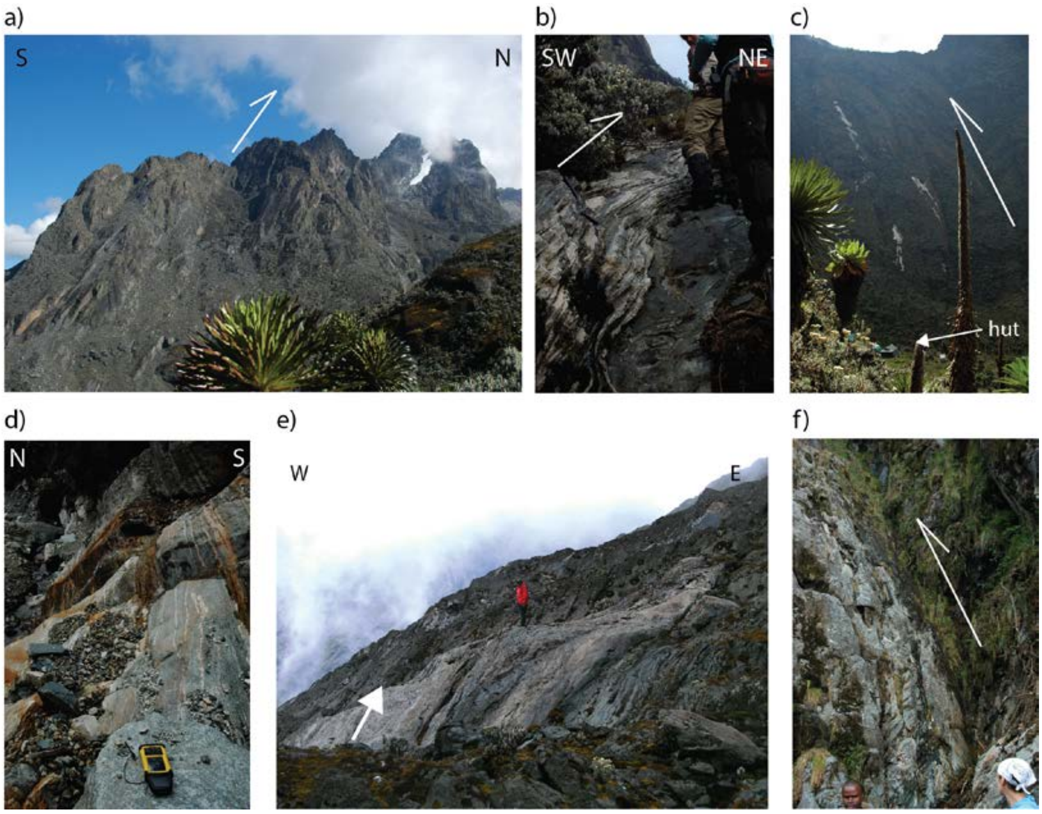

Figure 3 Photos of different fabrics in the high Rwenzori, figure locations are indicated in Fig. 2. a) Main southwards dipping fabric in the south of Mount Stanley seen from the east. b) Southwards dipping shear zone with quarzites

within the Mount Stanley amphibolites. c) Southwards dipping mylonite with a reverse sense of shear within the northern gneisses north of Bujuku hut. Reflecting surfaces represent the mylonite foliation and the arrow is pointing northwards. d) Greenschist facies shear zone within the northern schist unit below the amphibolites. e) Sheared calcsilicate layer (light grey rocks) within the amphibolites of mount Baker indicating north-directed thrusting. The white arrow shows the stretching lineation and indicates the transport direction. f) Late NW-wards directed brittle reverse faults on the trail from Nyabitaba to John Matte hut. The plane in the figure represents the fault surface.

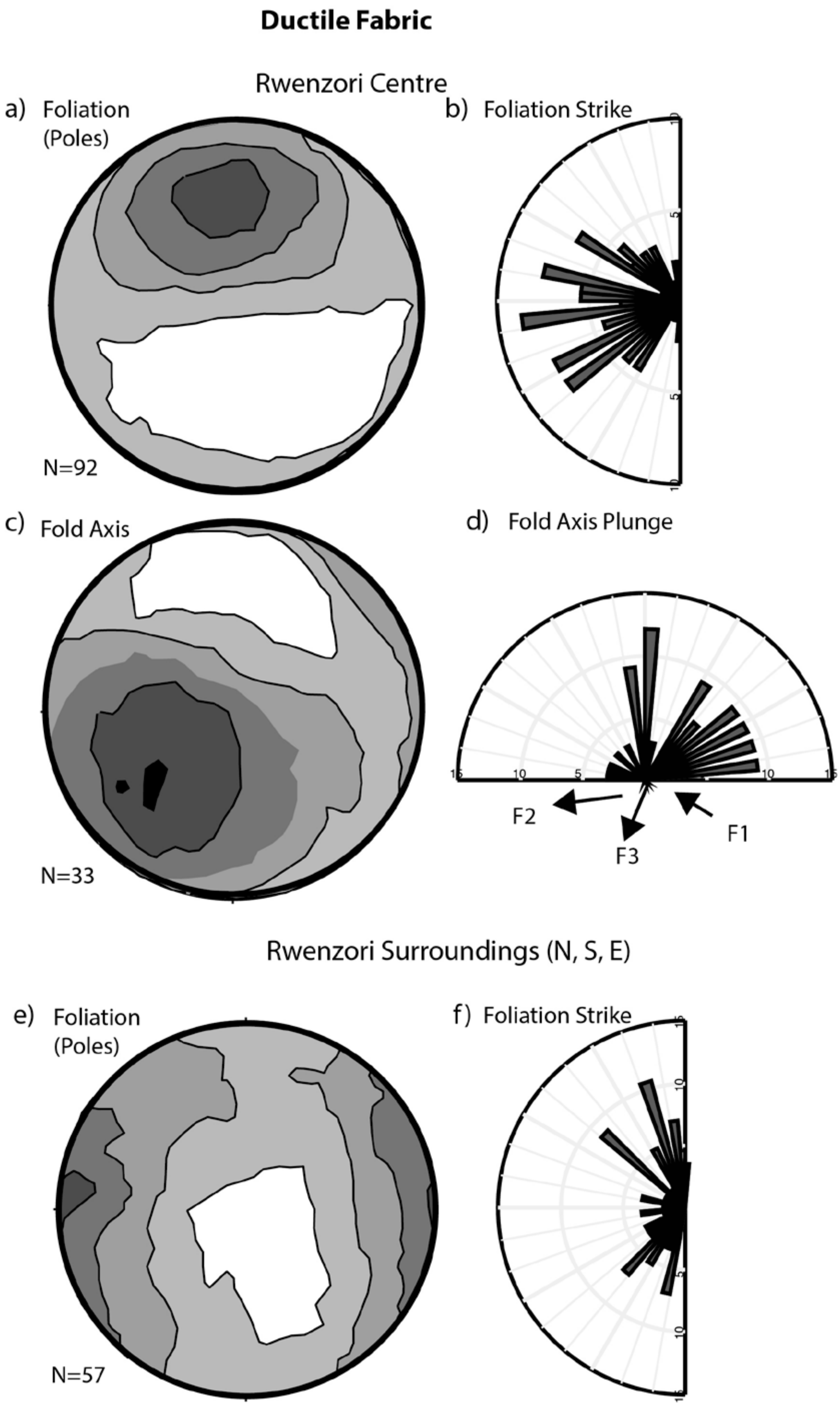

Figure 4 Plots showing ductile structures in the Rwenzori mountains. a) and b)

show foliation patterns within the central Rwenzori with a) a stereographic projection of poles to foliation with Kamb contours and b) rose diagrams of foliation strike. The dominantly southwards dipping fabric is evident in the plot. c) and d) show plunge and trend of fold axes within the central Rwenzori with c) Kamp contours of fold axes and d) a Rose diagram showing fold axis trend. c) shows mainly one major trend of fold axis, this represents mainly the D3 folding phase. However, the data is a mixture of D1, D2 and D3 folds, which can be seen better in the Rose diagram. e) and f) are poles to foliation and a Rose diagram of foliation strike in the north, east and south of the Rwenzori. The pattern is significantly different with a main NNW-SSE striking steep fabric. We acknowledge the use of the program Stereonet 6.3.2 from R.W. Allmendinger.

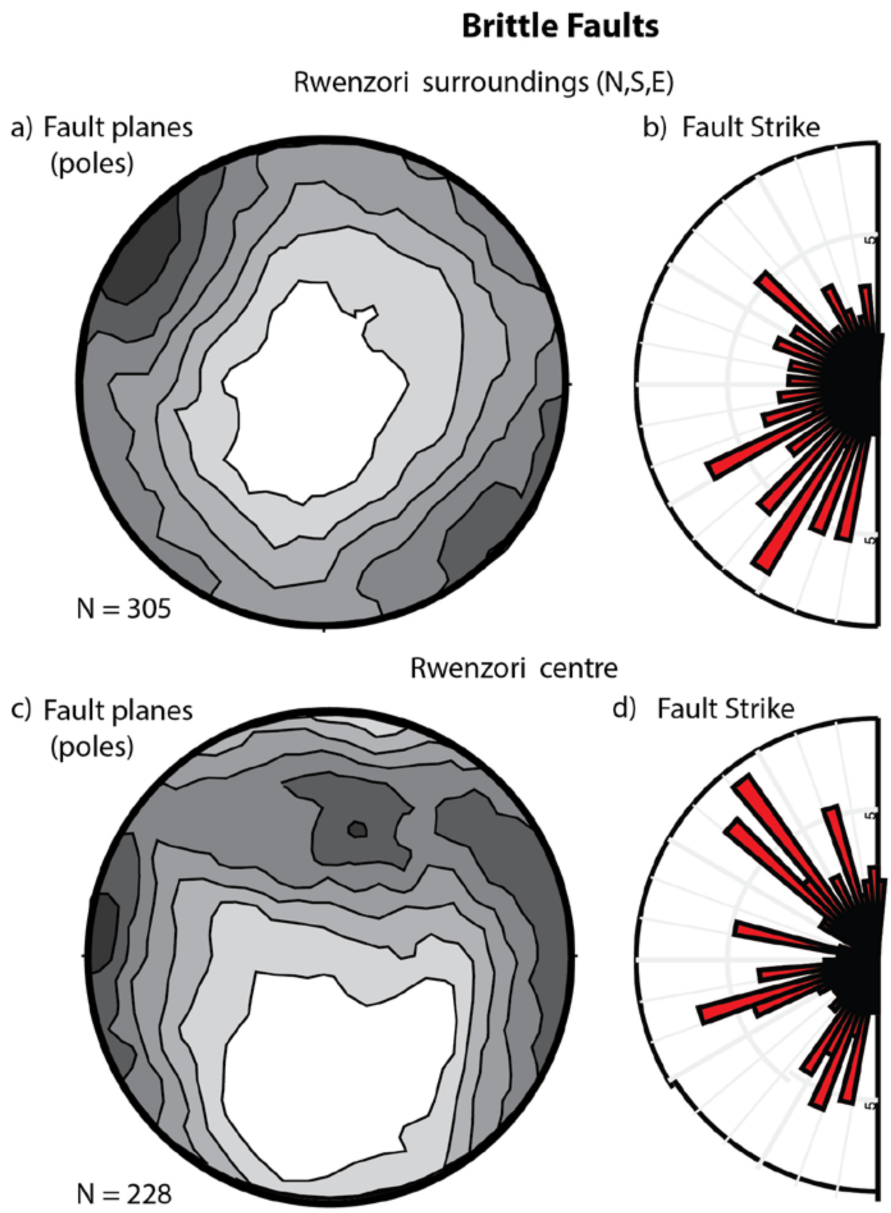

Figure 5 Brittle faults within the Rwenzori mountains. a) and b) faults within the north, east and south of the Rwenzori with a) poles to fault planes and b) a Rose diagram of fault strike. Two main directions emerge with steep faults that trend SW-NE and NW-SE. Note the difference to the trend of the ductile foliations. c) and d) show brittle faults in the high Rwenzori with c) Kamp contours of fault poles and d) Rose diagrams of fault strike. The main pattern that emerges is the southwards dipping fabric and two major steep fault trends with a NNW-SSE and a NNE-SSW trend. We acknowledge the use of the program Stereonet 6.3.2 from R.W. Allmendinger.

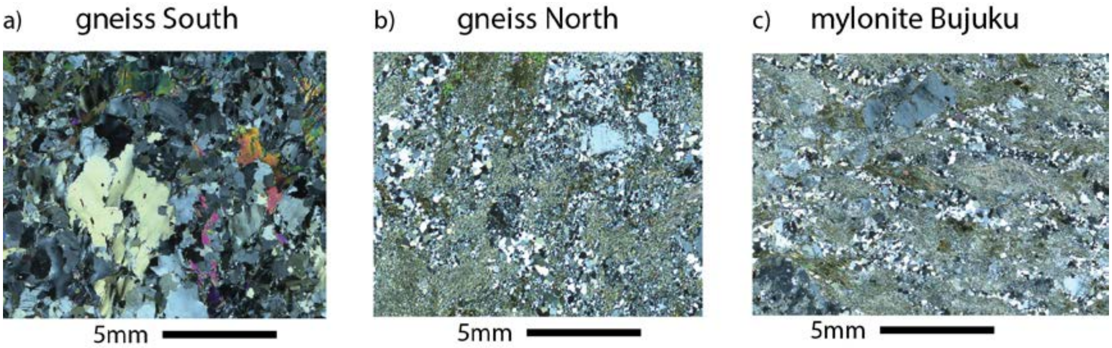

Figure 6 Thin section micrographs of the gneiss units in crossed polars with a) a thin section of the southern gneiss and b) and c) thin sections of the northern gneiss. The thin-sections show clearly different metamorphic conditions of the gneisses in a) and b) with the southern gneiss in a) showing amphibolite facies deformation features and large grains whereas the northern gneiss in (b) is recrystallized and shows greenschist facies conditions.

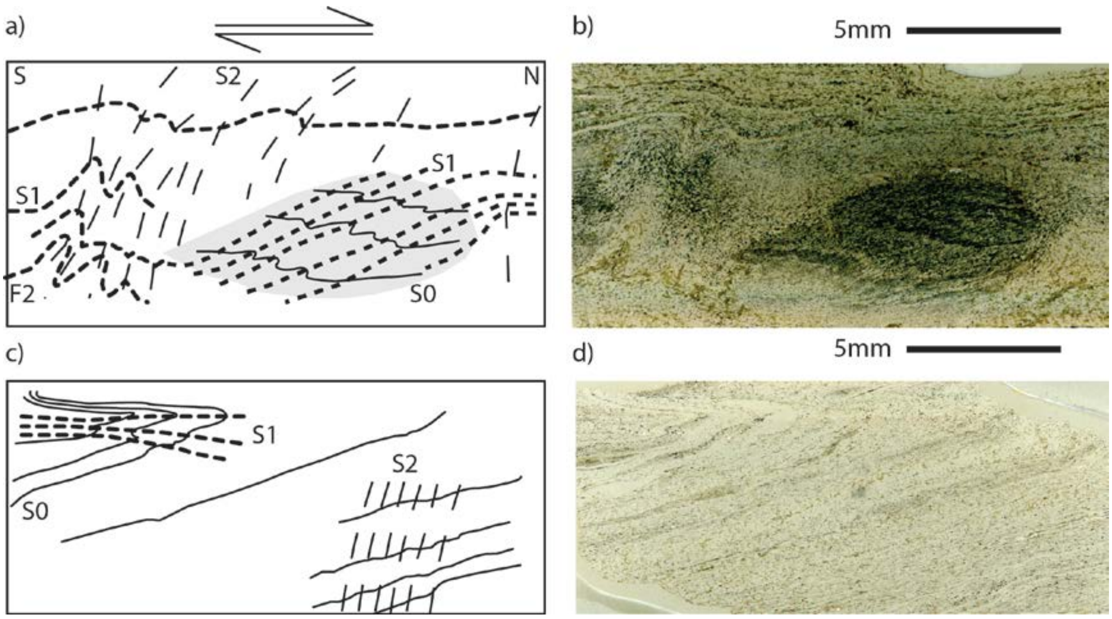

Figure 7 Thin section micrographs with the actual thin sections on the right hand side and interpretations of the fabric on the left hand side. The main deformation that can be seen is D1 and D2 with a large cordierite porphyroblast in b) showing overgrowth of D1 foliation and folding of S0.

F

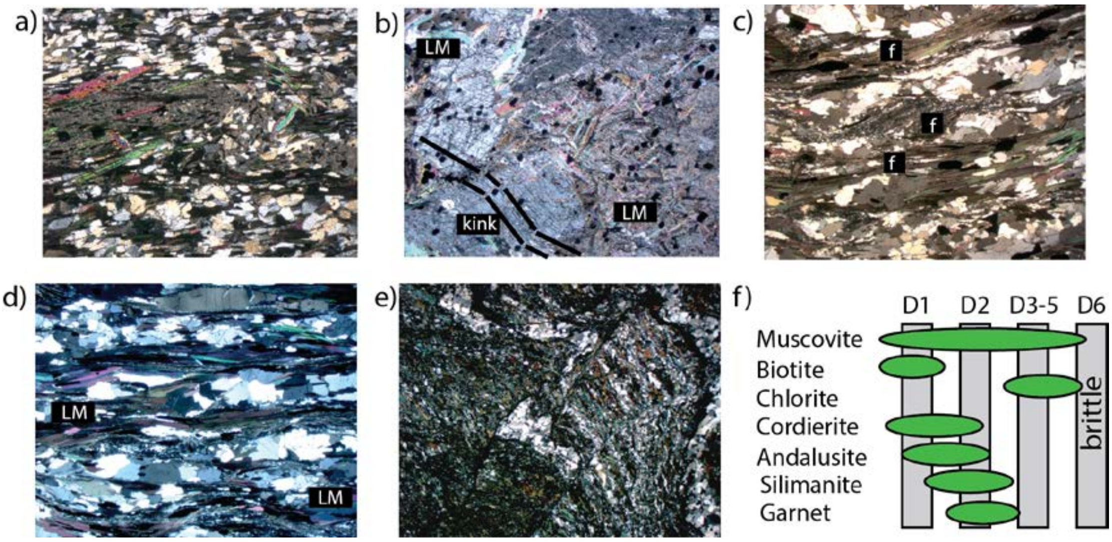

igure 8 Thin section micrographs of structures within the southern schist unit in a) to d), amphibolites in e) and an interpretation of the relation between metamorphic mineral growth and deformation in f). a) shows cordierte overgrowth on D1 folding, b) cordierte and andalusite overgrowth of D1 fabric, in addition to late mica (LM) c) fibrolitic silimanite (L) growth in D2 foliation, d) late muscovite growth and e) retrograde fabric representing the foliation of event D5. Thin-section photos have a width of 1cm. LM = late mica growth, f = fibrolite.

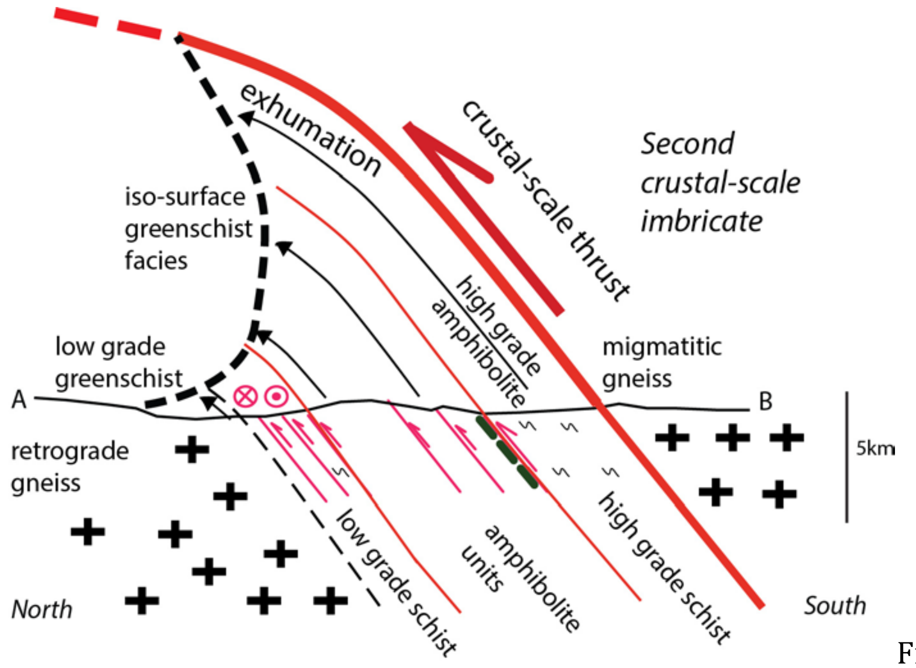

Figure 9

Interpretation of the Buganda-Toro belt in the central Rwenzori mountains. The inverse metamorphic grade is interpreted to be a function of an increase of shear and thus exhumation of deeper higher metamorphic units towards the south in the footwall of a crustal-scale thrust imbricate.